Proceedings of the Tenth Pacific Conference on Earthquake Engineering
Building an Earthquake-Resilient Pacific
6-8 November 2015, Sydney, Australia

Seismic assessment of CAMANAVA transportation lifelines using fragility analysis

M.B. Baylon & A.D. Co

Civil Engineering Department, College of Engineering,

University of the East – Caloocan, Samson Road, Caloocan City, Metro Manila, Philippines

ABSTRACT: A need for seismic assessment of important lifelines arises which could help in reducing seismic damages of the bridges and to inform citizens the danger they may encounter. The methodology employed in this paper included the modelling of the piers of some bridges and a fish port complex in CAMANAVA (Caloocan-Malabon-Navotas-Valenzuela) area using SAP2000 and used the peak ground acceleration gathered from PHIVOLCS, PEER, and K-Net (Kik-Net) as input data to the software to conduct analysis and determine whether horizontal or vertical ground motion will cause more damage to the structure. In this paper, SAP2000 was used in order to perform the Nonlinear Static Analysis (Pushover Analysis) and the Nonlinear Dynamic Analysis (Time History Analysis). The paper focuses and limits this study to determine whether the structure can withstand different PGAs that represents four (4) historical earthquakes. The final output were fragility curves which relate the probability of certain damages depending on different peak ground acceleration. As a result, the probability of occurrence of different peak ground accelerations from earthquakes affecting these lifelines will be addressed technically by declaring whether the pier columns analysed in the study will be affected or to what level the structural damage is.

1 INTRODUCTION

Seismic fragility is the probability that a geotechnical, structural, and/or non-structural system violates at least a limit state when subjected to a seismic event of specified intensity. Current methods for fragility analysis use peak ground acceleration (PGA), pseudo spectral acceleration (PSa), velocity (PSv), or spectral displacement (Sd) to characterize seismic intensity (Kafali & Grigoriu, 2004).

In establishing the seismic fragility curves, there is no universally applicable best method for calculating fragility curves (Requiso, Balili, & Garciano, 2013). The information that would be derived from the fragility curve can be used by design engineers, researchers, reliability experts, insurance experts and administrators of critical systems to analyze evaluate and improve the seismic performance of both structural and non-structural systems (Requiso D. A., 2013). In principle, the development of bridge fragility curves require the simultaneous use of the following methods: (1) professional judgment, (2) quasi-static and design code consistent analysis, (3) utilization of damage data associated with past earthquakes, and (4) numerical simulation of bridge seismic response based on structural dynamics (Shinozuka, Feng, Kim, Uzawa, & Ueda, 2003).

In the local setting, seismic assessment of bridge piers and a fish port was recently implemented by students in one of the universities in the country's capital. Their study was based from works of Karim-Yamazaki (2001), Shinozuka et. al (2003), and Ang-Park (1987) type of fragility curves with emphasis on the nonlinear static and nonlinear dynamic analyses.

This paper discusses the result of a research project done by groups of undergraduate civil engineering students whose objective is to accurately assess lifelines in the CAMANAVA (Caloocan-Malabon-Navotas-Valenzuela) area under various magnitudes of earthquakes. These lifelines that were studied are reinforced concrete deck girder bridge piers, fish port complex building columns, and light rail transit piers. The inputs of this research project are mainly initial and/or retrofitted structural plans from DPWH (Department of Public Works and Highways), LRTA (Light Rail Transit Authority) Depot, and respective city engineer's office. Ground motion data from PHIVOLCS (Philippine Institute of Volcanology and Seismology), PEER (Pacific Earthquake Engineering Research), and K-net.com were also collated. To process these data, both nonlinear analyses of structures were utilized; these are Pushover Analysis and Time History Analysis. The outputs are generated seismic fragility curves of the lifelines based from shear failure.

2 METHODOLOGY

For the purpose of developing a seismic fragility curve, two methods namely nonlinear static (Fig. 2) and nonlinear dynamic analysis (Fig. 3) were used to account for shear failure of one of its piers using SAP2000. Figure 1 illustrates how these two methods affect the construction of seismic fragility curves. This methodology will be applied repeatedly to the succeeding lifeline structures.

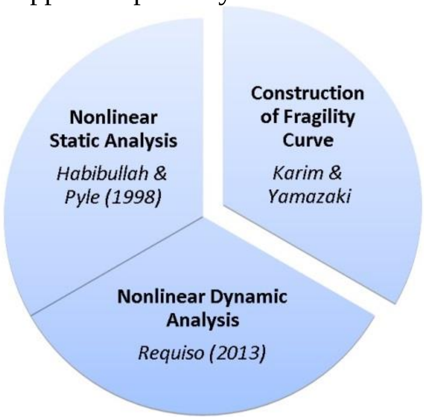

Figure 1. Methodology

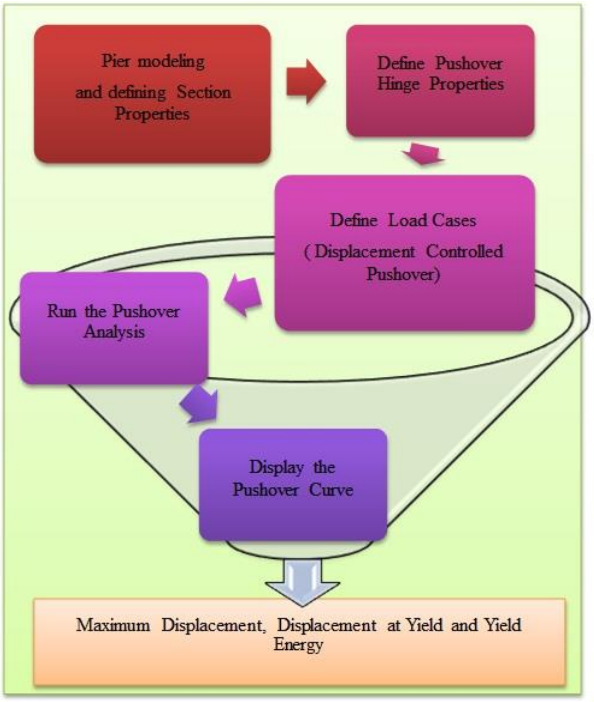

Figure 2. Nonlinear Static Analysis (Pushover analysis).

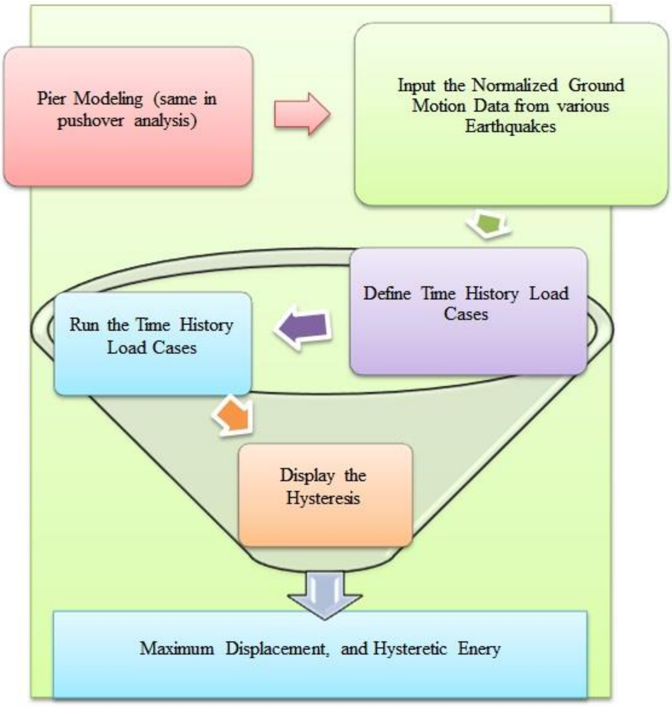

Figure 3. Nonlinear dynamic analysis (Time history analysis).

Using structural model of the building and normalized ground motion data as an input subjected to two nonlinear methods namely nonlinear static analysis and nonlinear dynamic analysis to develop seismic fragility curves. Peak Ground Acceleration (PGA) normalization is done by generating the original data to create another data for different PGAs. This is basically the same graph but different extent depending on the PGA. In the present study, the PGA normalization ranges from 0.2 g to 2.0 g.

In the present study, the author adapting the concept of time history analysis considering pier column as a single-degree-of-freedom (SDOF) system which is subjected to normalized ground motion having different excitations. In this paper, the ground motion records used were as follows:

Table 1. Summary of ground motion data used in this paper.

	Ground motion name	Station	Date of occurrence	Magnitude	Obtained from
1.	Tohoku-Kanto	Fukushima Station	March 11, 2011	9.0	Kik-net.com
2.	Tohoku-Kanto	AIC Station	March 11, 2011	9.0	Kik-net.com
3.	Tohoku-Kanto	HYG Station	March 11, 2011	9.0	Kik-net.com
4.	Tohoku	SIT Station	March 11, 2011	9.0	Kik-net.com
5.	Bohol	Quezon City Station	October 15, 2013	7.2	PHIVOLCS
6.	Mindoro	Cainta Rizal Station	November 15, 1994	7.1	PHIVOLCS
7.	Mindoro	Quezon City Station	November 15, 1994	7.1	PHIVOLCS
8.	Mindoro	Marikina Station	November 15, 1994	7.1	PHIVOLCS
9.	Kobe	Shin-Osaka Station	January 16, 1995	6.9	PEER
10	Kobe	Takarazuka Station	January 16, 1995	6.9	PEER
11	Kobe	Takatori Station	January 16, 1995	6.9	PEER
12	Kobe	Nishi-Akashi Station	January 16, 1995	6.9	PEER
13	Kobe	Kakogawa Station	January 16, 1995	6.9	PEER
14	Kobe	KJM Station	January 16, 1995	6.9	PEER
15	Kobe	HIK Station	January 16, 1995	6.9	PEER

The formula adapted from Karim and Yamazaki (2001) shown in Equation 1 where the ground motion data is multiplied by the ratio of the normalized and original peak ground acceleration defines the relationship of various earthquakes while maintaining its time history pattern.

$$\ddot{u}_{NEW} = A_0 \ddot{u}_{SOURCE} \tag{1}$$

Where:

$\ddot{u}_{NEW} = A_0 \ddot{u}_{SOURCE}$= the normalized groundmotion data.

$\ddot{u}_{SOURCE}$= the source groundmotion data.

A_0 =a coefficient factor to normalize the source of ground motion = $\dfrac{PGA_{normalized}}{PGA_{source}}$

Using software, the acceleration time histories obtained was used as an input producing another relationship between the force and displacement called the hysteresis model (bilinear model).

Nonlinear static analysis, also called as pushover analysis, is used to investigate the force-deformation behavior of a structure for a specified distribution of forces, typically lateral forces (Chopra, 2012). In this study, the pushover analysis is applied to produce pushover curve showing the relationship between the force and the displacement that would be used for further analysis.

From the output of the nonlinear static and nonlinear dynamic analyses which are the push-over curve and hysteresis model respectively, the ductility factors were obtained using the following equations, also adopted from Karim and Yamazaki (2001).

$$\mu_d = \frac{\delta_{\max}^{dynamic}}{\delta_y} \tag{2}$$

$$\mu_u = \frac{\delta_{\max}^{static}}{\delta_y} \tag{3}$$

$$\mu_h = \frac{E_h}{E_e} \tag{4}$$

Where:

μ_d= displacement ductility

μ_u= ultimate ductility

μ_h= hysteretic energy ductility

$\delta_{max}(static)$= displacement at maximum reaction at the push over curve (static)

$\delta_{max}(dynamic)$= maximum displacement at the hysteresis model (dynamic)

δ_y= yield displacement from the push-over curve (static)

E_h= hysteretic energy, i.e., area under the hysteresis model

E_e= yield energy, i.e., area under the push-over curve (static) but until yield point only

Once ductility factors are obtained, damage indices for the fragility curves can be determined using equation 5, taking β which is the cyclic loading factor as 0.15 according to Jiang, et. al (2012), for bridges. Again, this equation is credited to Karim-Yamazaki (2001).

$$I_D = \frac{\mu_d + \beta\mu_h}{\mu_u} \tag{5}$$

After computing the damage indices, damage rank for each damage index was determined using Table 6 or the HAZUS Damage Ranking.

3 RESULTS AND DISCUSSIONS

After obtaining the Pushover curve and the hysteresis models, one can now compute for the ductility factors. The yield point and the maximum displacement of the pushover curve can be located as illustrated in Fig. 4 and Table 2. The area under the pushover curve can be seen in Table 3.

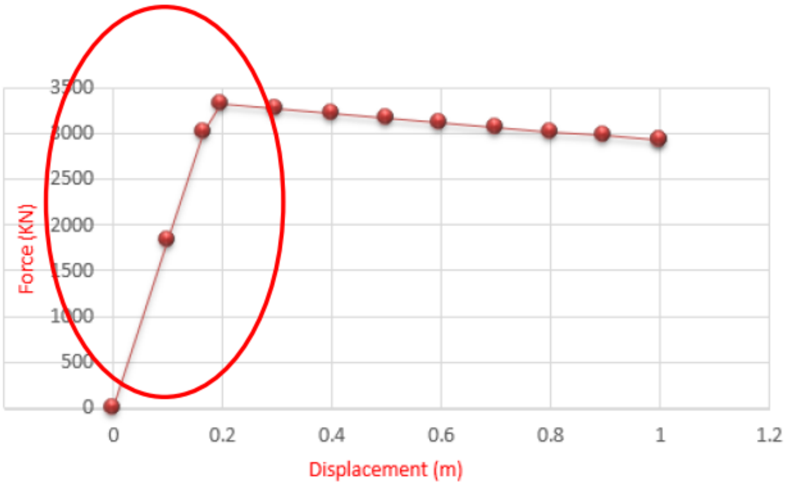

Figure 4. Pushover curve yield point and displacement.

Table 2. Pushover coordinates.

Step	Displacement m	BaseForce kN	Remarks
0	-1.483E-18	0	
1	0.1	1829.35	
2	0.164796	3014.70	← Yield point
3	0.196275	3316.17	← Maximum displacement
4	0.296275	3267.24	
5	0.396275	3218.30	
6	0.496275	3169.37	
7	0.596275	3120.43	
8	0.696275	3071.50	
9	0.796275	3022.56	
10	0.896275	2973.63	
11	0.996275	2924.70	
12	1	2922.87	

Table 3. Area under pushover curve (energy at yield point)

Formula	b	h	Ee
½ b h	0.164796	3014.7	248.4052506

The next step is to compute for the area of the hysteresis model (Figure 5) using the software AutoCAD.

Figure 5. Hysteresis Model using SAP2000.

After obtaining all parameters needed for ductility factors once can use Microsoft excel to compute the ductility factors up to damage indices. This can be seen in Table 4.

Table 4. Computation of Damage Index (DI) and Damage Rank (DR). e.g. Bohol Earthquake

PGA	STATIC NON-LINEAR ANALYSIS			DYNAMIC NON-LINEAR ANALYSIS			DUCTILITY FACTORS		DAMAGE INDEX	DAMAGE RANK
	δ_{max}	δ_y	E_e	δ_{max}	E_h	μ_d	μ_u	μ_h	(DI)	(DR)
0.2 g	0.196275	0.164796	248.40525	0.06143	5.291277011	0.372764	1.191018	0.021301	0.315662	C
0.4 g	0.196275	0.164796	248.40525	0.1228	21.16806174	0.745164	1.191018	0.085216	0.636385	B
0.6 g	0.196275	0.164796	248.40525	0.18429	47.65293468	1.118292	1.191018	0.191835	0.963098	A
0.8 g	0.196275	0.164796	248.40525	0.24563	84.71743748	1.490509	1.191018	0.341045	1.294411	As
1.0 g	0.196275	0.164796	248.40525	0.30709	132.3712585	1.863455	1.191018	0.532884	1.631703	As
1.2 g	0.196275	0.164796	248.40525	0.36846	190.6561724	2.235855	1.191018	0.767521	1.973928	As
1.4 g	0.196275	0.164796	248.40525	0.42995	259.0634974	2.608983	1.191018	1.042907	2.321895	As
1.6 g	0.196275	0.164796	248.40525	0.49131	338.8256055	2.981322	1.191018	1.364003	2.674958	As
1.8 g	0.196275	0.164796	248.40525	0.55278	429.4979965	3.354329	1.191018	1.729021	3.034112	As
2.0 g	0.196275	0.164796	248.40525	0.61434	529.0716826	3.727882	1.191018	2.129873	3.398238	As

By summing up all the counts of every damage index of every earthquake data as it can be seen in Table 4, one can compute for the damage ratio of each damage index which is summarized in Table 5 and can be illustrated in Fig. 6. The damage ranks were based from empirical values that relates a range of damage indices to an increasing rank of damages (HAZUS-MH, 2013). This table is reproduced in Table 6.

Table 5. All Earthquake Counts and Damage Ratios.

	COUNT						DAMAGE RATIO				
PGA	D	C	B	A	As		D	C	B	A	As
0.2 g	10	5	0	0	0	0.2 g	0.6666667	0.3333333	0	0	0
0.4 g	4	9	1	1	0	0.4 g	0.2666667	0.6	0.0666667	0.0666667	0
0.6 g	3	8	2	1	1	0.6 g	0.2	0.5333333	0.1333333	0.0666667	0.066667
0.8 g	3	5	2	3	2	0.8 g	0.2	0.3333333	0.1333333	0.2	0.133333

1.0 g	2	2	5	3	3	1.0 g	0.1333333	0.1333333	0.3333333	0.2	0.2
1.2 g	2	2	2	3	6	1.2 g	0.1333333	0.1333333	0.1333333	0.2	0.4
1.4 g	1	3	0	5	6	1.4 g	0.0666667	0.2	0	0.3333333	0.4
1.6 g	0	3	1	2	9	1.6 g	0	0.2	0.0666667	0.1333333	0.6
1.8 g	0	3	1	0	11	1.8 g	0	0.2	0.0666667	0	0.733333
2.0 g	0	3	1	0	11	2.0 g	0	0.2	0.0666667	0	0.733333

Table 6. Relationship between the damage index and damage rank based from HAZUS (2013).

Damage Index (DI)	Damage Rank (DR)	Definition
0.00 < DI ≤ 0.14	D	No damage
0.14< DI ≤ 0.40	C	Slight damage
0.40 < DI ≤ 0.60	B	Moderate damage
0.60 < DI ≤1.00	A	Extensive damage
1.00≤ DI	As	Complete damage

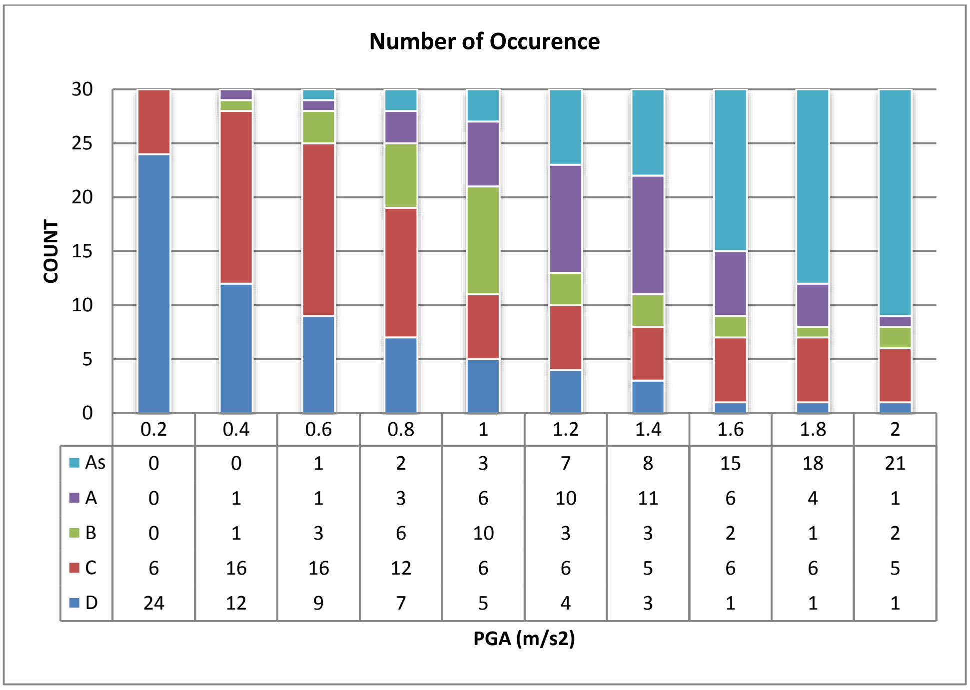

Figure 6. Frequency chart per damage rank.

The statistical formulas used in deriving the mean (λ) and standard deviation (ζ) were based from an ungrouped data premise.

$$\lambda = \frac{\sum_{i=1}^{N} f_i \cdot \ln(x_i)}{\sum_{i=1}^{N} f_i} \tag{6}$$

$$\zeta = \sqrt{\frac{\sum_{i=1}^{N} [\ln(x_i) - \lambda]^2}{N-1}} \tag{7}$$

Where:

f = frequency of damage rank per PGA.

x =the PGA in cm/s^2.
λ =the mean of the natural logarithm of PGA, in cm/s^2.
ζ =the standard deviation of the PGA, in cm/s^2.

Based from Equation 6 and Equation 7, Table 7 summarizes the results in computing the statistical parameters per damage rank that will be used later in deriving the probability of exceedance. The probability of exceedance in Equation 8 that was adapted in this paper is that of Karim-Yamazaki (2001).

$$P_r = \Phi\left[\frac{\ln(X)-\lambda}{\zeta}\right] \tag{8}$$

Where:

P_r =Cumulative Probability of Exceedance
Φ = Cumulative Normal Distribution Function
X = Peak Ground Acceleration
λ = Mean
ζ = Standard Deviation

Table 7. Tabulation of the statistical parameters to be used in the plotting of fragility curves.

Damage Ratio	D	C	B	A	As
Mean	1.495912761	1.981027686	2.27510658	2.433917553	2.658697831
Standard D.	0.734910121	0.642327251	0.369400506	0.30889602	0.249402945

Table 8. Summary of probability of exceedance per damage rank (DR)

PGA (in g)	D	C	B	A	As
0.2	0	0.02093	0.00001	0.00000	0.00000
0.4	0.43044	0.16959	0.00699	0.00028	0.00000
0.6	0.64671	0.37277	0.08685	0.01614	0.00019
0.8	0.77873	0.54909	0.28041	0.11320	0.00821
1	0.85804	0.68109	0.50896	0.31303	0.06619
1.2	0.90652	0.77475	0.69708	0.54101	0.21954
1.4	0.93692	0.84003	0.82467	0.72641	0.43815
1.6	0.95647	0.88541	0.90231	0.84950	0.64793
1.8	0.96935	0.9171	0.9467	0.92155	0.80289
2	0.97803	0.93941	0.97121	0.96051	0.89875

By using lognormal distribution one can compute for the "P_r" or the Probability of exceedance. Then one can plot the acquired cumulative probability with the peak ground acceleration (PGA) normalized to different excitation.

In the fragility analysis, the mathematical definition of fragility function in Equation 9, that is adapted in this paper, is a conditional probability of a structure that will experience a certain damage rank given an intensity measure based from an assumed mode of damage. This conditional probability can be expressed mathematically in Equation 4.

$$P_R = P(D < C | IM) \tag{9}$$

Where:

P_R = probability of exceedance

D = demand, in this case, the base shear

C = capacity, in this case, the shear capacity of the pier column

IM = intensity measure, in this case, the peak ground acceleration, PGA.

The fragility curve can now be obtained as in Figure 7 of the seismic fragility curves of Tullahan-Ugong bridge. This fragility curve is based from Table 8.

The above procedure was repeated for the rest of the lifeline structures and can be summarized by the following charts. In Fig. 8, the fragility curves of the lifelines are plotted when DR='C' or equivalent to Slightly Damage. This is followed by charts of Figures 9, 10, and 11 which correspond to Damage Ranks B, A, and As, respectively. These fragility curves data were from the results of the undergraduate theses of Alcaraz et. al. (2015), Algura et. al. (2015), Canlas et. al. (2015), Cruz et. al. (2015) and Del Carmen et. al. (2015).

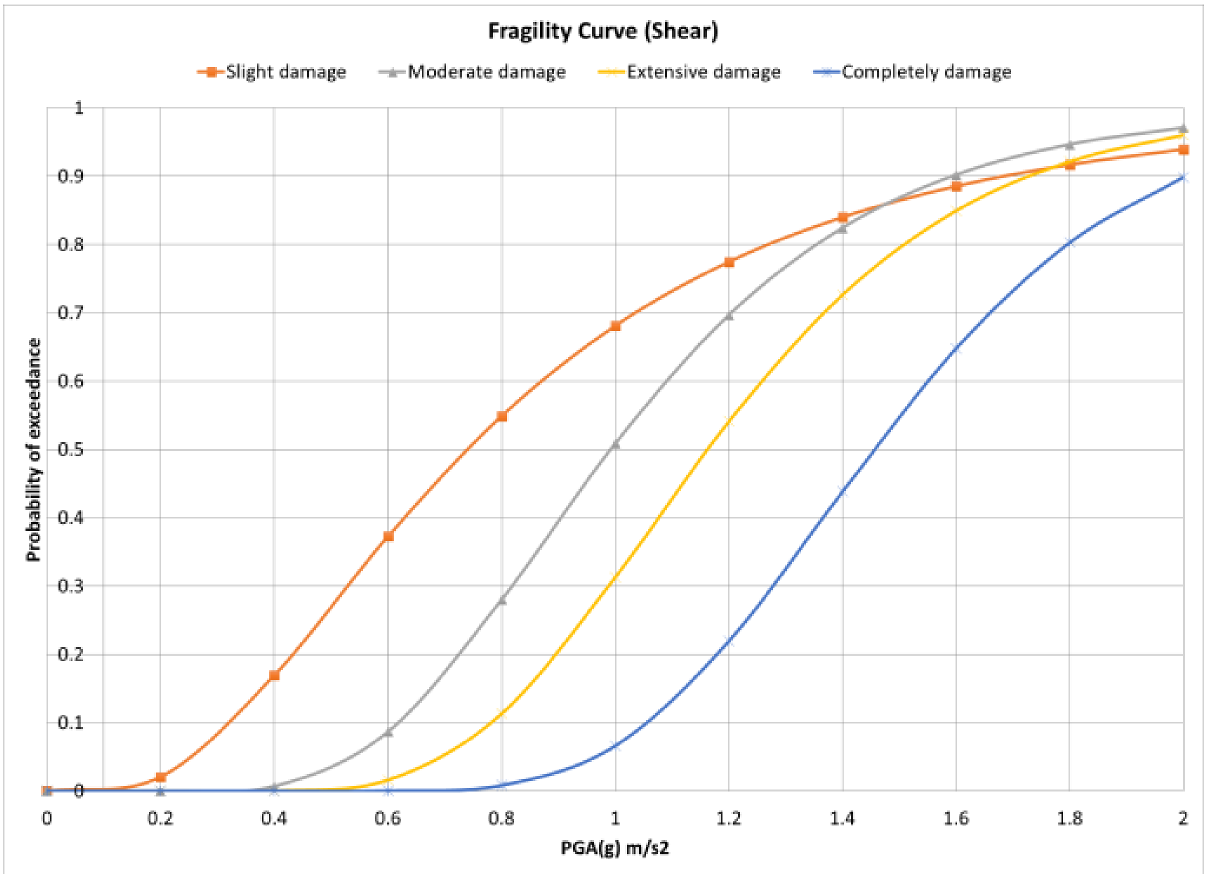

Figure 7. Seismic Fragility Curves of Tullahan-Ugong Bridge.

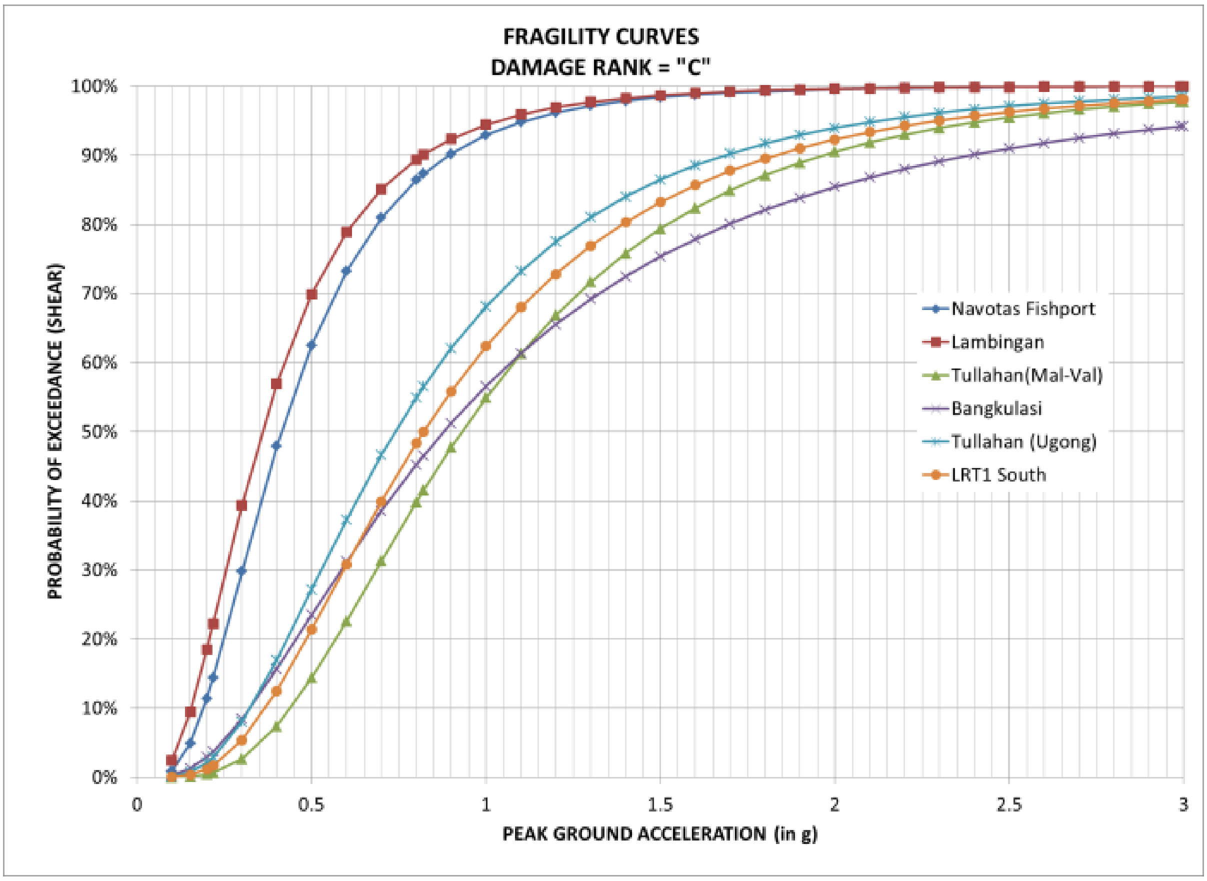

Figure 8. Fragility curves of Damage Rank C or Slight Damage.

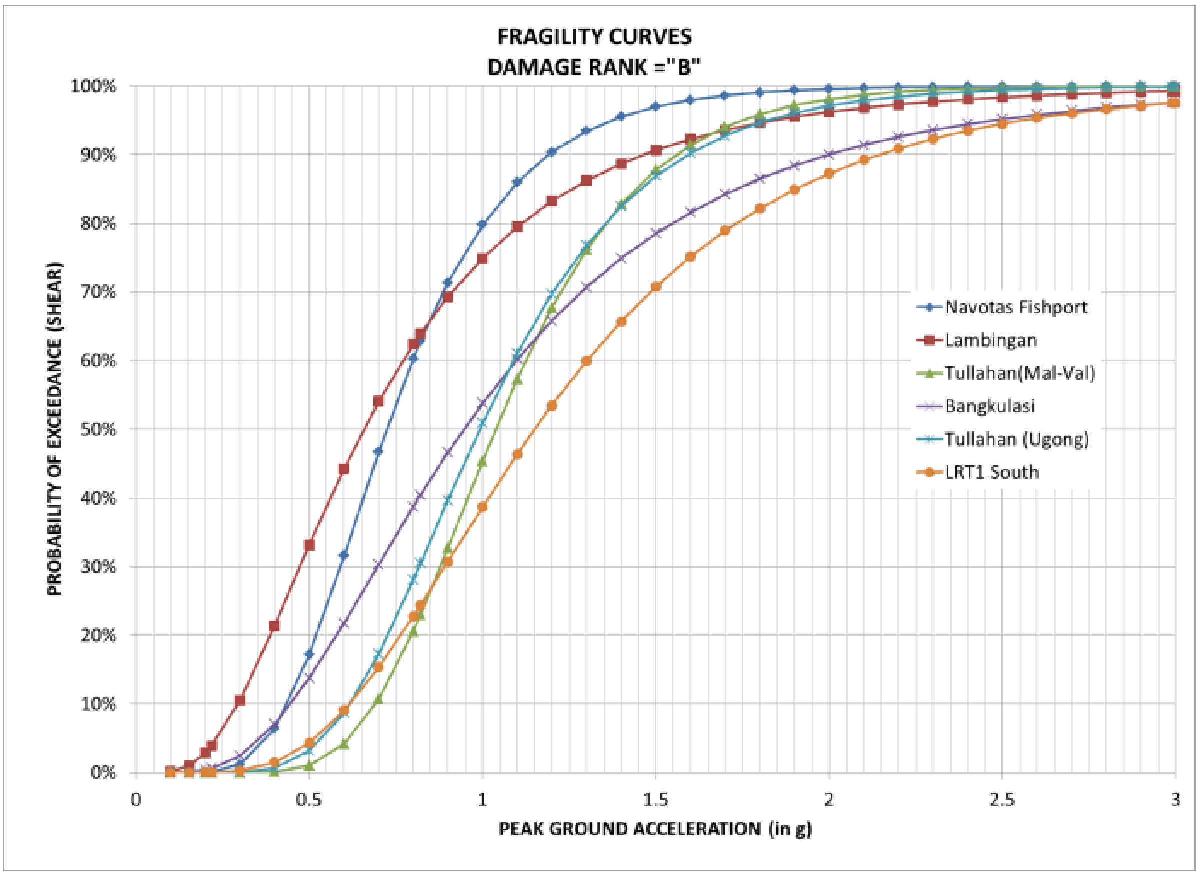

Figure 9. Fragility curves of Damage Rank B or Moderate Damage.

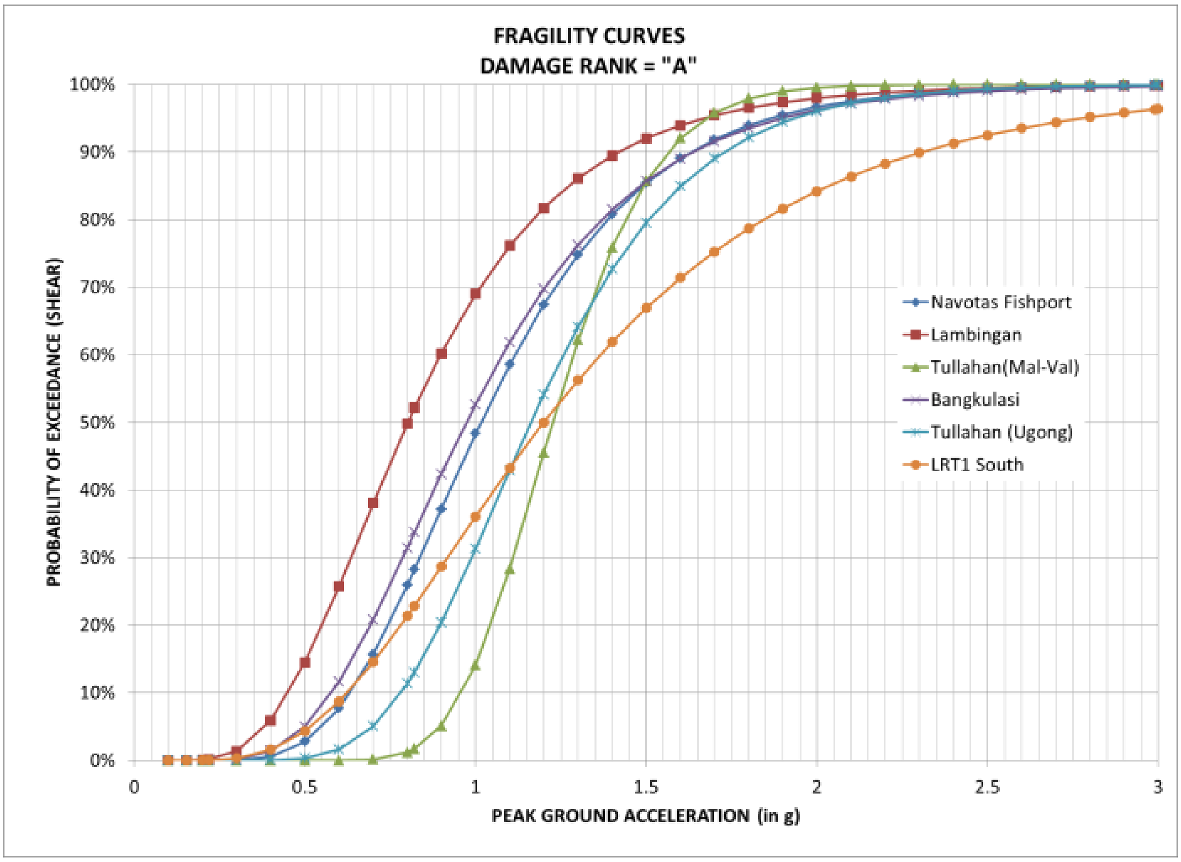

Figure 10. Fragility curves of Damage Rank A or Extensive Damage.

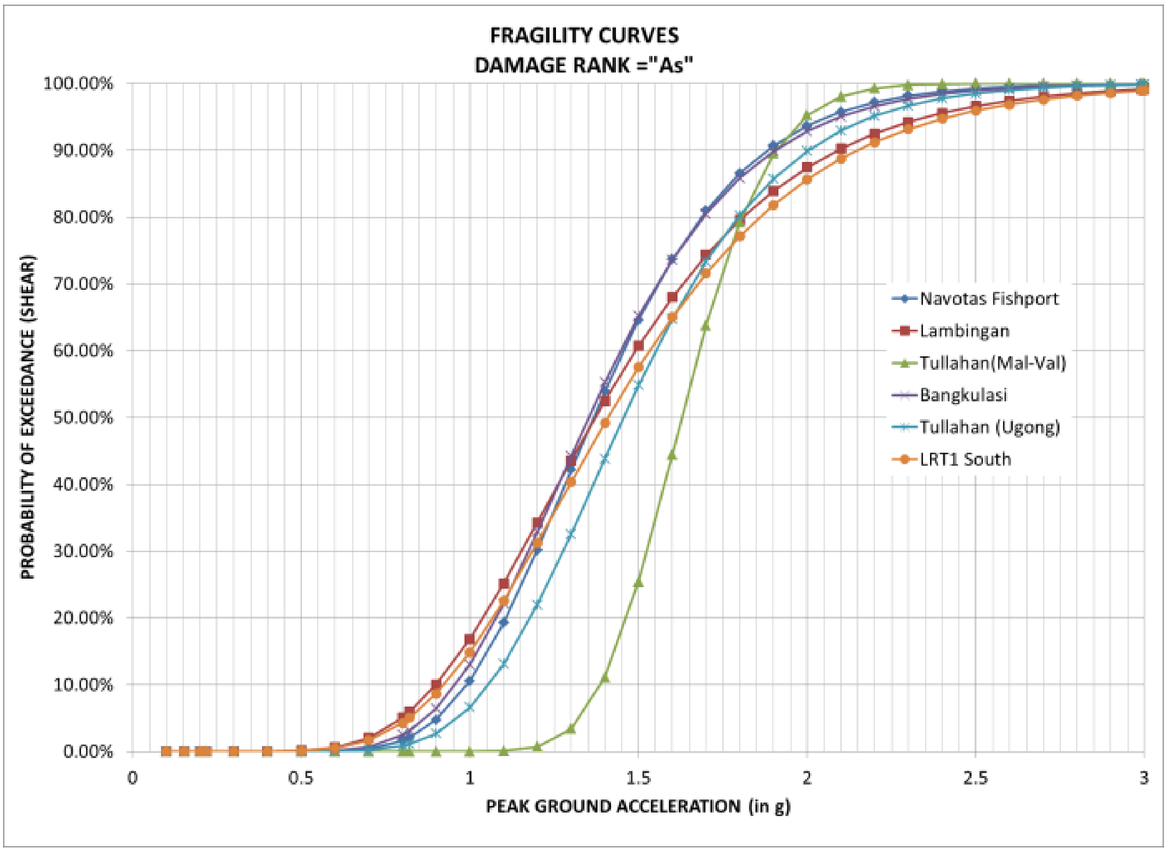

Figure 11. Fragility curves of Damage Rank As or Complete Damage

From the fragility curves that were developed, it can be seen that each damage rank increase from different peak ground acceleration. There is a low possibility that the bridge will be completely damaged at a peak ground acceleration of 0.7g, it also shows that the curve for completely damage gradually increase at approximately 0.8g, these data suggests that the piers of the bridge is sufficiently safe from completely damage since it requires larger earthquake shaking to cause significant damage.

The bridge piers are not spared from being damaged. It can be observed that the piers already have a slightly damage at 0.2g, but none of these damage ranks are able to produce a 100% probability of exceedance.

4 CONCLUSION AND RECOMMENDATION

This paper discusses the fragility curve as an effective tool for analyzing, designing, and evaluation of a structure that subjected to an earthquake. It can be used as an effective tool for visualizing the effect of an earthquake to lifelines such as bridges, light rail transit, and fish port complex structure, by knowing their response to earthquake. One can tell how much it has been damaged if an earthquake occurs. It can be seen that the bridge piers are still safe from shear failure since it requires a larger earthquake shaking to cause significant damage and these results gives us proof to its structural safety and serviceability.

5 REFERENCES

Alcaraz, R. P., Cuadra, C. J., & Damian, R. S. (2015). *Seismic assessment of Navotas fish port complex.* Caloocan: Undergraduate Thesis; University of the East - Caloocan.

Algura, D. O., Decal, A., Quilang, J. R., & Romero, E. J. (2015). *Seismic Assessment of Tullahan Bridge (Malabon-Valenzuela).* Caloocan: Undergraduate Thesis; University of the East - Caloocan.

Ang, A. H., & Tang, W. H. (2007). *Probability Concepts in Engineering: Emphasis on Applications to Civil and Environmental Engineering Volume 1 (2nd ed.).* New Jersey: John Wiley & Sons, Inc.

Baylon, M. B. (2015). Seismic assessment of transportation lifeline in Metro Manila. *2nd CAMANAVA Studies Conference* (pp. 1-7). Caloocan: University of the East - Caloocan.

Canlas, L., Mallanao, R. N., San Diego, A., & Santiago, M. A. (2015). *Seismic assessment of Bangkulasi bridge piers.* Caloocan: Undergraduate Thesis; University of the East - Caloocan.

Choi, E., DesRoches, R., & Nielson, B. (2004). Seismic fragility of typical bridges in moderate seismic zones. *Engineering Structures*, 187-199.

Chopra, A. K. (2012). *Dynamic of Structures (Theory and Applicationsto Earthquake Engineering).* United States of America: Pearson Education, Inc.

Cruz, F. G., Gueco, F. E., Matammu, D. L., & Maglanoc, B. S. (2015). *Seismic assessment of Tullahan-Ugong bridge piers due to shear failure using fragility curves (Caloocan-Valenzuela)* . Caloocan: Undergraduate Thesis; University of the East - Caloocan.

Del Carmen, M. O., Kakilala, M., Santos, K., & Vicedo, N. (2015). *Seismic assessment of Light Rail Transit Line 1 South Extension.* Caloocan: Undergraduate Thesis; University of the East - Caloocan.

Gomez, H., Torbol, M., & Feng, M. (2013). Fragility analysis of highway bridges based on long-term monitoring data. *Computer-Aided Civil and Infrastructure Engineering*.

HAZUS-MH. (2013, July 26). Retrieved September 04, 2015, from A Federal Emergency Management Agency Website: http://www.fema.gov/media-library-data/20130726-1716-25045-6422/hazus_mr4_earthquake_tech_manual.pdf

Jernigan, J., & Hwang, H. (2002). Development of bridge fagility curves. *7th US National Conference on Earthquake Engineering.* Boston, Massachusetts: EERI.

Jiang, H., Fu, B., Lu, X., & Chen, L. (2012). Constant - damage Yield Strength Spectra. *15th World Conference on Earthquake Engineering.* Lisbon.

Kafali, C., & Grigoriu, M. (2004). Seismic fragility analysis. *9th ASCE Specialty Conference on Probabilistic Mechanics and Structural Reliability*. USA: ASCE.

Karim, K. R., & Yamazaki, F. (2001). Effect of Earthquake Ground Motions on Frgility Curves of Highway Bridge Piers Based on Numerical Simulation. *Earthquake Engineering and Structural Dynamics*.

Krawinkler, H., & Seneviratna. (1998). Pros and cons of a pushover analysis of sesmic performance evaluation. *Engineering Structures Vol. 20 Nos. 4-6*, 452-464.

Nielson, B. G. (2005). *Analytical fragility curves for highway bridgesi in moderate seismic zones.* Atlanta: Doctor of Philiosophy Dissertation; Georgia Institute of Technology.

Nowak, A. S., & Collins, K. R. (2013). *Reliability of structures.* Boca Raton, Florida: CRC Press.

Park, Y. J., Ang, A. H.-S., & Wen, Y. K. (1987). Damage limiting a seismic design of buildings. *Earthquake Spectra*, *3*(1), 1-26.

Park, Y.-J., & Ang, A. H.-S. (1985). Mechanistic Seismic Damage Model for Reinforced Concrete. *ASCE Journal of Structural Engineering , 111*(4), 722–739.

Requiso, D. A. (2013). *The generation of fragility curves of a pier under high magnitude earthquakes (a case study of the metro rail transit-3 pier).* Manila: Undergraduate Thesis; De La Salle University.

Requiso, D. T., Balili, A., & Garciano, L. E. (2013). Development of seismic fragility curves of a transportation lifeline pier in the Philippines. *16th ASEP International Convention.* Makati: Association of Structural Engineers of the Philippines, Inc.

Shinozuka, M., Feng, M. Q., Kim, H., Uzawa, T., & Ueda, T. (2003). *Statistical Analysis of Fragility Curves*. MCEER.